

# Towards Electrically-Pumped AlGaN UV-A Lasers with Transparent Tunnel Junctions

Arnob Ghosh<sup>1</sup>, Agnes M. D. M. Xavier<sup>1</sup>, Sheikh Ifatur Rahman<sup>1</sup>, Andrew Allerman<sup>3</sup>, Siddharth Rajan<sup>1,2</sup> and Shamsul Arafin<sup>1</sup>

<sup>1</sup>Department of Electrical and Computer Engineering, The Ohio State University, Columbus, OH 43210, USA

<sup>2</sup>Department of Materials Science and Engineering, The Ohio State University, Columbus, OH 43210, USA

<sup>3</sup>Sandia National Laboratories, Albuquerque, New Mexico 87185, USA

\*Email: [arafin.1@osu.edu](mailto:arafin.1@osu.edu)

**Abstract:** Molecular beam epitaxy-grown GaN/AlGaN-based active regions were optimized by varying quantum-well widths to yield increased photoluminescence intensity at UV-A wavelengths. The optimized gain medium was then used in electrically-pumped laser structures with transparent tunnel junctions. © 2023 The Author(s)

AlGaN-based ultraviolet (UV) lasers have attracted tremendous interests due to their potential applications including air- and water-purification, disinfection, sterilization, fluorescence spectroscopy, and laser lithography. Despite of few reports on electrically-pumped AlGaN based UV-A lasers under pulsed conditions [1,2], continuous-wave operation in this wavelength regime is not yet achieved primarily due to high threshold current caused by poor doping and resulting low conductivity and high absorption in *p*-layers. A promising way to circumvent the problem is the use of a homojunction tunnel junction (HJ-TJ) [3]. Another important parameter for AlGaN lasers is the quantum well (QW) thickness which influences the threshold current due to presence of the quantum confined stark effect (QCSE). In this work, we report the design, growth and fabrication of GaN/AlGaN based laser materials with a buried tunnel junction and an optimized active region emitting around 355 nm.

The active region for lasers used in the study consists of a single GaN QW and Al<sub>0.2</sub>Ga<sub>0.8</sub>N barriers. The materials were grown by plasma assisted molecular beam epitaxy (PAMBE). For optimizing the active region, several test photoluminescence (PL) structures with varying GaN well thicknesses were grown on *n*-doped Al<sub>0.3</sub>Ga<sub>0.7</sub>N templates-on-sapphire substrates. Fig. 1(a) represents the cross-sectional schematics of the three PL structures which are labelled as sample-A, -B and -C. Fig. 1(b) shows the room temperature PL spectra of the three samples. The dominant peak at 355 nm observed from sample-A with a well thickness of 2.4 nm originates from  $E_{c1}-E_{hh1}$  transition of the QW which is in good agreement with the calculated value using the 6-band *k.p* model. The calculated band diagram considering all the polarization charges originated at the GaN/AlGaN hetero interface for only sample-A is shown in Fig. 1(c). The strain of GaN/AlGaN QW in this structure is compressive in nature, which gives rise to large polarization fields and quantum confined stark effect and thus reduces the overlap between electron and hole wave function. With increased well thickness, the electron-hole separation further increases, which reduces the emission

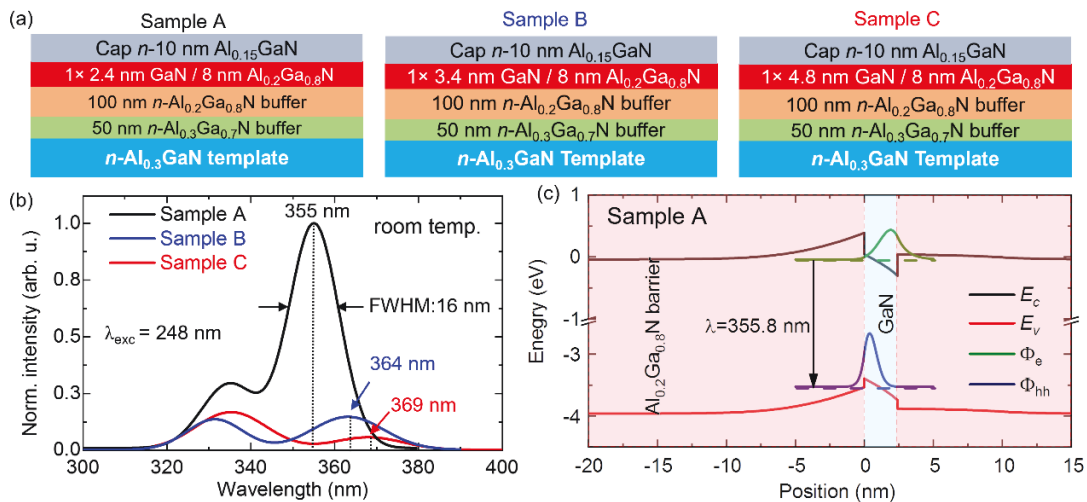


Fig. 1 (a). Schematic of the structures used for PL study, (b) Band diagram of the structure in sample A calculated using 6 band *k.p* model and (c) Room-temperature PL spectrum for the quantum wells with different well thickness.

energy even below the bulk bandgap and increases the linewidth of the emission spectrum. This is also evident from the PL spectra obtained from sample-B and -C with a well thickness of 3.4 nm and 4.8 nm, respectively. As the well width increases, the peak wavelength shifts to 364 nm and 369 nm for the sample-B and -C, respectively. Their full width half maximum also increase. The second peak at 335 nm was obtained from all three samples which is believed to be originated from the  $\text{Al}_{0.15}\text{Ga}_{0.85}\text{N}$  cap layer. Based on the PL intensity, sample-A was chosen to demonstrate electrically-pumped lasers. It should be noted that further decreasing the well thickness will lead to poor carrier confinement reducing the emission intensity.

The laser epitaxial materials, as shown in Fig. 2(a), was then grown on the same template used for the PL study. The laser structure consists of a 300-nm-thick  $\text{Al}_{0.3}\text{Ga}_{0.7}\text{N}$   $n$ -doped cladding layer followed by an active region consisting of a single 2.4 nm GaN QW and 60 nm  $\text{Al}_{0.2}\text{Ga}_{0.8}\text{N}$  waveguide layer on top and bottom. A 10 nm  $p$  doped  $\text{Al}_{0.4}\text{Ga}_{0.6}\text{N}$  layer was used as an electron blocking layer (EBL). A homojunction tunnel junction was grown on top of this EBL with highly doped  $p^{++}$  layer graded down from  $\text{Al}_{0.3\rightarrow 0.2}\text{Ga}_{0.7\rightarrow 0.8}\text{N}$  and then a highly doped  $n^{++}$  layer graded up from  $\text{Al}_{0.2\rightarrow 0.3}\text{Ga}_{0.8\rightarrow 0.7}\text{N}$  on the  $n$ -side to take advantage of the induced 3D polarization charge. On top of the tunnel-junction, 300 nm  $\text{Al}_{0.3}\text{Ga}_{0.7}\text{N}$   $n$ -doped cladding was grown. The growth was ended by 15 nm heavily doped  $n^{++}\text{Al}_{0.3}\text{Ga}_{0.7}\text{N}$  top contact layer. The band diagram of the laser structure is shown in Fig. 2(b). The spatial mode profile for the structure was also calculated. The composition of each layer was extracted from the  $2\theta$ - $\omega$  scan by XRD as shown in Fig. 2(c) which closely matches with the composition of the designed structure. From the reciprocal space mapping data, shown in Fig. 2(d), it is visible that the waveguide layer and the cladding layers are strained to the template composition. The surface morphology studied by atomic force microscopy is presented in Fig. 2(e) shows step-flow growth features with a surface roughness of 1.4 nm. The benefit of such a design is that now both the top and bottom contacts can be formed on  $n$ - $\text{Al}_{0.3}\text{Ga}_{0.7}\text{N}$  layers which eliminates the need of a  $p$ -GaN layer or  $p$ -AlGaN/GaN superlattice giving superiority over conventional lasers. To evaluate the electrical characteristics of the device, Ti/Al/Ni/Au contact was deposited on top of the  $p$ -contact layer and the bottom  $n$ -templates by opening an  $80\ \mu\text{m}$  square mesa defined by dry etching. The current-voltage characteristic is shown in Fig. 2(f) where a voltage drop of 5 V at  $20\ \text{Acm}^{-2}$  is seen.

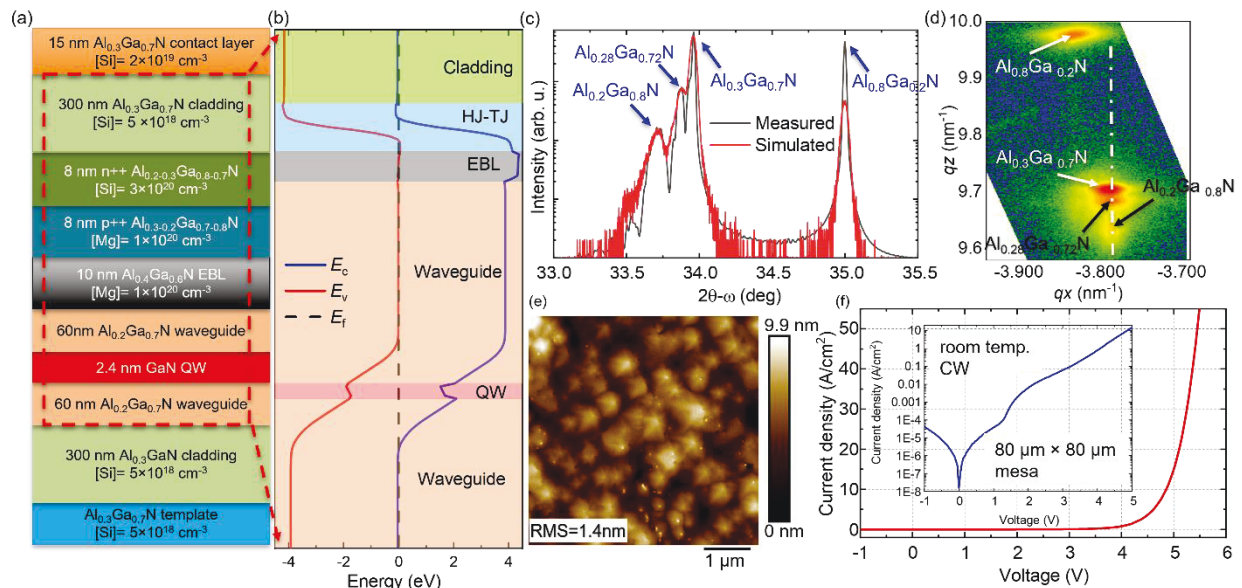


Fig. 2 (a). Schematic of the designed laser structure (b) band diagram of the laser material stack (c) extracted composition of different layers from XRD  $2\theta$ - $\omega$  scan. (d) reciprocal space mapping (e)  $5\ \mu\text{m} \times 5\ \mu\text{m}$  atomic force microscopy image of the surface of the laser epitaxial layer stack. (f) current voltage characteristic

Our work reports the growth, fabrication and characterization of GaN/AlGaN laser materials with a buried tunnel junction and optimized active region for the emission around 355 nm. Complete growth details with advanced material characterization of optimized narrow ridge laser fabrication process will be presented in the conference.

This research was funded by the National Science Foundation under grant number 2034140.

## References

- [1] H. Yoshida, *et al.*, "A 342-nm ultraviolet AlGaIn multiple quantum-well laser diode," *Nat. Photon.* **2**, 551-554 (2008).
- [2] Y. Aoki, *et al.*, "A 350-nm-band GaN/AlGaIn multiple-quantum-well laser diode on bulk GaN," *Appl. Phys. Lett.* **107**, 151103 (2015).
- [3] S. Krishnamoorthy, *et al.*, "Polarization-engineered GaN/InGaIn/GaN tunnel diodes," *Appl. Phys. Lett.* **97**, 203502 (2010).